Construction Robotics (2022) 6:319–328
https://doi.org/10.1007/s41693-022-00086-z

ORIGINAL PAPER

A modified common midpoint approach for GPR radars

Davide Picchi[1] · **Sigrid Brell-Çokcan**[1]

Received: 16 September 2022 / Accepted: 25 November 2022 / Published online: 25 December 2022

Abstract
Ground Penetrating Radar (GPR) plays an important role among the non-destructive methods used to analyze, measure and collect data from pavement layers, building structures and archaeological sites. A GPR device consists of a radar able to get an image, technically called radargram, of the subsurface. Due to the decreasing costs of calculation power, it is now possible to analyze and interpret radargrams more efficiently than in past. While technological advancements and improvements in the post-processing of data have increased the power of this process, it is also important to consider survey technique as a key factor in nondestructive testing. The aim of this paper is to propose a modification of a well-known survey technique called Common Mid-Point (CMP). The conventional CMP survey technique requires that the transmitter and receiver of the GPR device be physically separated to survey a site. This provides the benefit of determining the speed of light in the host medium from the slant of the hyperbola reflection of a buried target. The CMP process unifies the inspection technology into a single device, making the use of GPR more accessible to robots on construction sites. The method documented in this paper is based on a mathematical model for adapting the conventional CMP for conventional GPR radar devices, in which transmitter and receiver cannot be separated physically.

Keywords Ground penetrating radar · Signal processing · Common midpoint · GPR survey

1 Introduction

The principle behind GPRradar devices is to measure the amplitude of a reflected signal versus time after the signal is emitted from the transmitting antenna. The reflected signal can be measured in time-domain or in frequency-domain, according to the specific device used (Harry 2009). However, the time-domain approach is more intuitive to be understood and read by a human operator. GPRradar devices were originally deployed to gather position information and location data about buried objects in the ground as well as to analyse the layer consistency of pavements like asphalt roads and others relevant sites in the discipline of civil engineering (Daniels 2005) (Greaves 2009). The development of such devices and related techniques increased in the last decades to such a point that GPRis now extensively used as a non-destructive method for building and construction inspections. this technology has been deployed in the investigation of structural integrity on projects ranging from bridges, runway, roads, buildings and archaeological site. The benefit of this approach extends to additional disciplines including archaeology, sedimentology, glaciology and other geophysical engineering applications (Harry 2009). The following two factors have contributed to this wide range of use cases: the development and research in High Frequency (HF) technology led to a miniaturization of electronics devices and microprocessors in the last decades. The introduction of smaller, more efficient antennas also led to a reduction in size of GPRdevices. Small devices can be now stored in a small case and transported directly to the survey site. The downside of this reduction of the antenna size is that higher frequencies must be utilized as the antenna dimensions and geometry determines the wavelength of the transmitted and received signals. The use of higher frequencies has a positive effect in that the resolution of the collected radargrams is improved as compared to lower frequencies. While the better resolution of a radargram is a positive factor, the trade-off

Sigrid Brell-Çokcan contributed equally to this work.

✉ Davide Picchi
picchi@ip.rwth-aachen.de

Sigrid Brell-Çokcan
brell-cokcan@ip.rwth-aachen.de

[1] Individualized Production, RWTH-Aachen University, Campus Boulevard 30, 52074 Aachen, Germany

is that higher frequencies result in a reduction of the scanning depth (Takahashi 2012, Harry (2009). The development of more powerful post-processing algorithms led to an increased ability to analyse more complex site structures and radar data (Harry 2009). Through these improved post-processing algorithms, professional tools are capable of achieving a 3D reconstruction of the site data collected by a GPRdevice and underlying structures (Shan and Imad 2016).

While commercial devices often include connections to proprietary software for post-processing, the development of algorithms for research purposes should be independent (agnostic) from the adopted survey technique. This offers the biggest flexibility to analyse and extract features from the radar data without restrictions due to proprietary software. The electromagnetic properties of the site material (in this research referred to as the host medium) have a big impact on the propagation of radar signals (Shan and Imad 2016), Daniels (2005), especially on the field properties of the reflected signal like: velocity of propagation, signal attenuation and wave impedance (Harry 2009). One of the most challenging questions then is how to estimate or determine the electromagnetic properties of the host medium using GPRradar relying only on the measure of the reflected wave, without any other devices or destructive methods. A traditional GPRdevice can measure the *time of flight*, *the frequency* and the *amplitude* of the reflected signal (Harry 2009), but is unable to output directly the thickness of the underlying host medium or the depth of a buried object for following reasons: the first reason is that the electromagnetic properties of the host medium are *a priori* unknown. This means that obtaining the depth of a buried object or a thickness of the host medium cannot be retrieved by measuring the properties of the reflected signal wave, since those properties depend on the electromagnetic properties of the host medium itself. Secondly, the host medium could be not homogeneous or could show a multilayer structure. This leads to the problem, that many unknown factors need to be taken into consideration (e.g., how many different layers are present in the host medium, differences from different measure points, etc.) (Harry 2009). Third, all electromagnetic waves properties of a signal exhibit similar behaviours but the propagation of a wave in a host medium depends strongly on the dielectric, magnetic and conductive properties of the host medium itself (Harry 2009), which are dependent on the frequency of the exciting signal. Given a buried object in a host medium and a GPRdevice, then setting different emitting frequencies, leads to different results, even if the depth of the buried object never changed during the survey. This effect should be taken into account, when using different GPRdevices and/or comparing surveys, where the peak frequency is differently set.

The depth of a buried object can be estimated once the operator knows exactly through which medium the signal is going to propagate. This leads to the biggest dilemma in the GPRfield: a knowledge of the electromagnetic properties of a medium is vital to estimate how far a radar wave can propagate, but the electromagnetic properties are, in many cases, *a priori* not known. For this reason, many techniques have been developed to allow for a first estimation of the signal propagation in the host medium. Once the light speed in the medium has been estimated, it is possible to get an estimation of the depth at which a buried object has been detected. Under the assumption, that a signal path spreads radially from a transmitting antenna and knowing the distance between transmitter and receiver, it is possible to apply some geometrical rules to estimate with a good approximation the depth of the buried object.

The use of robots in construction requires close collaboration between automation equipment, sensors and humans. In order to utilize robots on dynamic construction sites it is necessary to not only integrate sensors but adapt them for automated processes. The challenge of using robots with current forms of GPRis that multiple robots would be required to precisely synchronize movements of the sender and receiver. The following paper documents the development of a new method for GPRwhich unifies the process into a single device capable of sending and receiving. In this way a single construction robot would be capable of utilizing GPRto inspect as built construction before robotic processes are engaged. The following innovation allow for a more accessible approach to GPRenabling the integration of the sensor into a mobile collaborative platform for use in robotic inspection. This opens the possibility of combining human robot collaboration with automated concrete inspection. The scope of this paper focuses on the new form of GPRas a step towards a more automated capability between human, robot and inspection sensors on construction sites.

2 Methods

GPRradar technology can be applied to estimate the depth of a buried object or the layer thickness of a host medium, by measuring the time interval between the emitted signal and the received wave once reflected from the buried object or any interface with a material with different relative permittivity. Different procedures have been developed since the introduction of GPRradar in the geophysical field. The common mid-point (CMP) and the wide-angle reflection and refraction (WARR) are two examples of conceptually similar operation modi for the estimation of the seismic light of speed in a host medium (Harry 2009). There are some procedures like transillumination surveys, where transmitter and receiver are put into boreholes, but since the aim of this research is non-destructive methods, such transillumination techniques are not taken into account. Furthermore, WARR

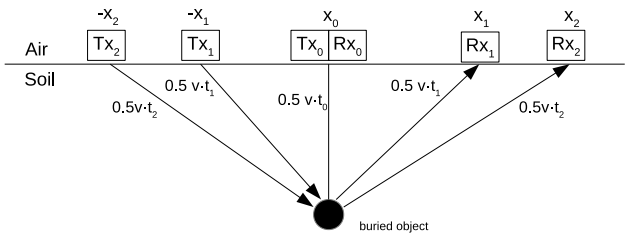

Fig. 1 Schema of a conventional CMP measurement

operation modi is more suitable for geophysical applications (White 2020) while the first method (CMP) is suitable for building structures (Persico 2014). Conventional CMP procedures, as in Fig. 1, make use of a transmitter and receiver, which are moved on a surface at predefined steps along the X axis (parallel to the soil) symmetrically to a common point of origin x_0. Because the length of the path traveled by the signal is symmetrical to the vertical axis (crossing x_0), the time of flight t_n, which is the time sent by the transmitter and captured by the receiver, is simply halved from transmitter to the target and from the target to the receiver.

In order to determine the speed of the light in host medium (which is the key to get the relative permittivity of the soil) the following trigonometrical relations of a right-angled triangle can be applied:

$$vt_n = 2\sqrt{(x - x_0)^2 + \left(\frac{vt_0}{2}\right)^2} \tag{1}$$

This process uses the same calculation schema proposed in Persico (Persico 2014), where: the time of flight of the signal t_n is the time the signal needs from the transmitter and back to the receiver, while t_0 is the time to and from the target at the coordinate of the minimum distance (x_0). The benefits of the CMP procedure is that the receiver does not saturate when receiving the reflected signal (Persico 2014). The constraint is that the process requires more time to survey a site, since transmitter and receiver must be moved independently from each other for every scan (Persico 2014).

Further constraints arise in the utilization of GPRdevices embedded into a closed case as commonly found in the construction industry. The form of these devices limit the possible distance between transmitter and receiver units. While this allows for convenience user operation, it limits the possibility of applying CMP techniques, which leverage the greater distance between signal source and receiving sensor (e.g., the GPRdevice from the company GSSI in FIg. 2). The device in Fig. 2 is an example of a GPRradar, where the distance between transmitter and receiver is fixed and cannot be modify.

The following research details a proposed approach for addressing this process constraint. Since the proposed

Fig. 2 Structure Scan Mini: a GPRdevice from GSSI developed for building structures

approach changes the common CMP calculation method by just swapping the time of flight of the signal between different scan positions, the approach taken into consideration is the time-domain approach. The idea expressed in this paper aim to mathematically integrate the benefit of GPR devices with fixed distance between transmitter and receiver units. By adapting calculation methods this research seeks to close the gap between processes without requiring new hardware. The following section introduce the mathematical concepts, and detail simulation experiments carried out to validate the proposed method before summarizing the research in consideration of future developments.

3 Proposed procedure

In this paper a virtual host medium with homogeneous electromagnetic characteristics has been considered and the basic principles of CMP are illustrated. The program *gprMax* (Warren et al. 2016) has been extensively used for simulations. This program lets the user run simulations in an environment which is highly configurable through text-based scripting and can output all the required signal properties: time of flight, the electromagnetic fields of the signal and the position of the antenna. The results of the simulation are visualized using the *Matlab*© tools available with the program or using a *HDF5* library available for *Python*. *Python* has been used extensively in this research, as it offers benefits at the prototyping level being an accessible powerful scripting language. Additionally, the use of *Python* allows for the possibility to run the same script on a majority of

computers, allowing for serialization of different input data and the execution of simulations (e.g., moving merged files, once a simulation has finished, starting a new simulation, incrementally changing parameters for new simulations, etc.). As *gprMax* is written in *Python* it is relatively straightforward to implement a *Python* script which collects *gprMax* system calls and post-process data of the simulation outputs. Other assumptions made in this study include:

- The relative permittivity ϵ_r and the magnetic loss σ_* of the host medium are constant. This means, that the host medium can be represented as a single layer of material with homogeneous characteristics
- Conductivity σ and the relative permeability μ_r of the host medium are neglected, since they do not have any influence on the process demonstration shown in this study
- The antenna used for the simulation is not a virtualization of a real one, but an abstraction of a transmitting source and receiving unit: a hertzian dipole. Even if the program allows simulating an environment with Bowtie or other real antennas, the choice of a hertzian dipole has the advantage to speed up simulations focusing only on their results. First attempts have been conducted using a bowtie antenna model, but simulation times grew to a level, where single simulation runs took almost half a day on a recent high powerful computer to be carried out
- The simulated GPRdevice is ground-coupled. This assumption lead to a simulation result, where there are no electromagnetic effects between ground surfaces and antennas, since the distance between them is zero
- The excitation signal from transmitter is a *Ricker* wavelet with a peak frequency $f = 1.5$ GHz. Future simulations will investigate the proposed procedure using different source waveforms and evaluating the difference between them, if any
- The considered system (composed of transmitting and receiving unit) is bistatic. That means, that two different antennas are implemented in the simulation environment. One antenna is used for transmitting, while the second antenna is used for receiving
- The accuracy of the generated signal *could* be modeled in the script to take into account the noise sensor and make the simulations closer to real situations. Different simulations done before this paper showed that, many initial conditions (position of the radar in the simulated environment, the space resolution of *gprMax*, the frequency used, the electromagnetic properties of the soil and the type of radio-wave used in the simulation, etc.) affect very deeply the results of the simulations. For this reason, the noise of the sensor has been neglected for this work, but surely considered for further developments and in more complex environment sceneries.

In consideration of a GPRunit where transmitter and receiver are integrated and not separable, then a possible survey pattern would be represented by the diagram shown in Fig. 3, where the first scan begins on the left and then the device is moved to right side by a constant step.

At regular intervals the time of flight of the signal t_n (the time flight of the signal at the position x_n) is being read as in the schema in Table 1 and according to the publication (Liang et al. 2020):

At this point an important consideration should be taken into account. The offset between transmitter and the receiver *could* be set to zero in the simulation environment, since the used hertzian dipole does not really depict a real antenna. But, since in a real GPRsystem an offset between transmitter and receiver is expected to be not zero, it makes sense to consider at first a system, where the offset a is small but not zero and

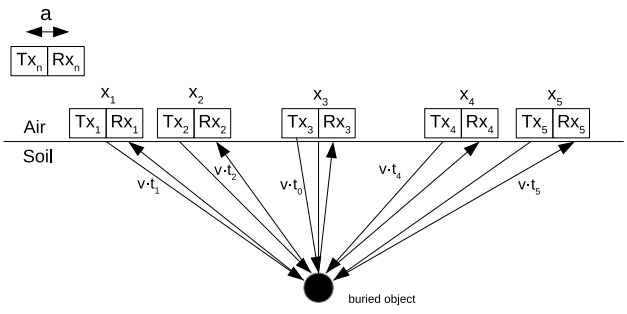

Fig. 3 Survey pattern with a GPRdevice. Transmitter and receiver are not separable

Table 1 Table reflecting the schema of Fig. 3

Scan	*X* axis coordinate	t [ns]
1	x_1	t_1
2	x_2	t_2
3	x_3	t_3
4	x_4	t_4
5	x_5	t_5

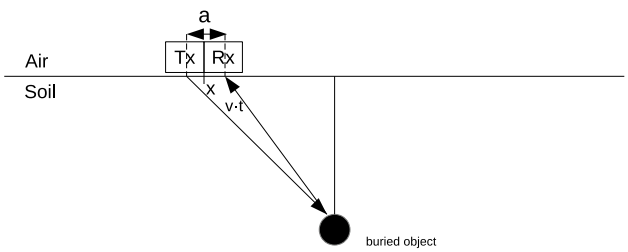

Fig. 4 Offset between transmitter and receiver in a real antenna

then to evaluate, which impact such offset has on the estimation of travel time of a signal (Fig. 4).

With reference to Persico (2014) for the interfacial data in common offset mode with a non-null offset, the equation describing the travel time of a signal in Fig. 4 is expressed as:

$$vt_n = \sqrt{\left(x - x_0 - \frac{a}{2}\right)^2 + \left(\frac{vt_0}{2}\right)^2 - \left(\frac{a}{2}\right)^2} + \sqrt{\left(x - x_0 + \frac{a}{2}\right)^2 + \left(\frac{vt_0}{2}\right)^2 - \left(\frac{a}{2}\right)^2} \tag{2}$$

where a is the offset between transmitter and receiver and x is the coordinate of the midpoint between transmitter and receiver. For this reason the position of the transmitter can be calculated as: $(x - a/2)$ and the position of the receiver as $(x + a/2)$: .

Neglecting the offset a the Eq. 2 yields to Eq. 1, which imply a simplification of the mathematical model. After executing some simulations to verify, whether it is possible or not, to approximate that equation, it was found that the offsets used for the simulations can be neglected. So Eq. 1 can be used to estimate the speed of light v in the host medium.

A better look to the Fig. 5, where the transmitted and the reflected signal are shown separately, shows that the signal is composed by the combination of two different components:

- The time of flight from transmitter to the target: t_t
- The time of flight from target to the receiver: t_r

The sum of both travel times yield to the measured travel time and can be simply expressed by the following equation:

$$t_n = t_t + t_r \tag{3}$$

Since neglecting the offset a between transmitter and receiver, the travel paths in Fig. 5 overlap, it is acceptable to assume that:

$$t_t = t_r \tag{4}$$

therefore:

$$t_n = 2t_t = 2t_r \tag{5}$$

where t_n is the total travel time of the signal. Under the assumption that the scans are taken symmetrically to the vertical axis, where the distance between surface and the target is at a minimum ($z = 0.5vt_0$ on Fig. 6), then the resulting scan schema does not really differ from the original CMP technique procedure (Fig. 1). The only condition to be met, is that the scan order and its travel time need to be resorted, in order to apply the same CMP calculation method, even if the device used does not allow for any separation between transmitter and receiver.

Back to Fig. 1, the scan sequence and the corresponding travel time of the signal t_n can be ordered in a vector:

$$\mathbf{x} = \{x_0, (-x_1, x_1), (-x_2, x_2)\} \tag{6}$$

$$\mathbf{CMP} = [t_0, t_1, t_2] \tag{7}$$

On the other side a survey with a GPRdevice, where transmitter and receiver are inseparable, the scan order sequence (as in Fig. 6) can be expressed by a vector as well:

$$\mathbf{x} = \{x_1, x_2, x_3, x_4, x_5\} \tag{8}$$

$$\mathbf{CMP_{mod}} = [t_1, t_2, t_3, t_4, t_5] \tag{9}$$

Due to the symmetry of the scan pattern explained in this section and considering that:

$$x_1 = x_5, x_2 = x_4, x_3 = x_0 \tag{10}$$

$$t_1 = t_5, t_2 = t_4, t_3 = t_0 \tag{11}$$

after substitution the vector x and the vector $\mathbf{CMP_{mod}}$ can be rewritten as:

$$\mathbf{CMP_{mod}} = [t_1, t_2, t_0, t_2, t_1] \tag{12}$$

and a sort of the columns leads to:

$$\mathbf{x} = \{x_0, (x_2, x_4), (x_1, x_5)\} \tag{13}$$

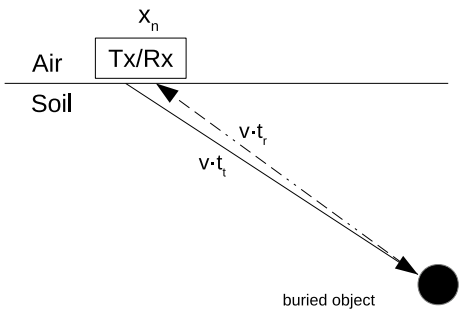

Fig. 5 Travel path of a signal of a monostatic antenna system

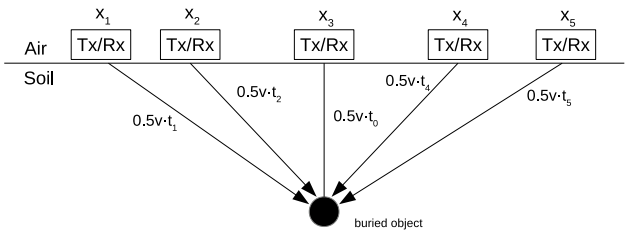

Fig. 6 Schema of the modified CMP technique. The return path of the signal from the target to the receiver is not shown, since it overlaps with the ongoing signal

$$\mathbf{CMP_{mod}} = [t_0, t_1, t_2] = \mathbf{CMP} \tag{14}$$

In others words: under the assumption of GPRsystem, where transmitter and receiver are inseparable, and a survey pattern is symmetrical to the vertical axis, it is possible to apply the same known CMP technique for the estimation of the relative permittivity of the host medium. Since the output of a scanning survey can be seen as matrix form (where every column represents a single A-scan), it is simply necessary to sort the columns (or the rows) of the resulting matrix in order to apply the CMP algorithm calculation. The following Fig. 7 shows an example of a resulting B-scan taken from a simulation, where a conventional CMP survey technique has been carried out. The travel time is minimum at the beginning of the survey (position x_0) and then rises as transmitter and receiver move away from each other. On the other side, the travel time of a signal reaches its minimum, once a GPRdevice (inseparable Tx/Rx) is exactly on the top of the buried object, as a look to Fig. 7 can confirm.

In the following section, simulations are carried out in order to evaluate the calculation pattern explained in this paper. The following pseudocode (Algorithm 1) resembles the concept expressed in this chapter.

Algorithm 1 CMP modified procedure

```
procedure CMP
    pos = [x_1, x_2, ..., x_n]
    t = [t_1, t_2, ..., t_n]
    t_0, index = min(t)
    x_0 = pos[index]

    if len(t) is even then
        print ← "Even number of measurements"
    else
        counter = 0
        x_r = {x_0}
        t_r = {t_0}

        while (index − counter) >= 0 and (index + counter) <= len(t) + 1
    do
            x[counter] = pos[index − counter]
            t[counter] = t[index − counter]
            conter + = 1
        end while
    end if
    sort(x_r)
    sort(t_r)
    return x_r, t_r
end procedure
```

4 Simulations

As mentioned in section proposed procedure the Finite-Difference Time-Domain (FDTD) simulation program *gprMax* has been used for simulating and evaluating the survey procedure explained above. A simple air-ground model with a buried metal bar in a host medium has been implemented as a script and then run in the *gprMax* environment. The host medium has the dimensions: 2.0 x 3.0 x 0.002 m, while the metallic bar has the dimensions: 0.02 x 0.01 x 0.002 m. The distance between the upper side of the metallic bar and the

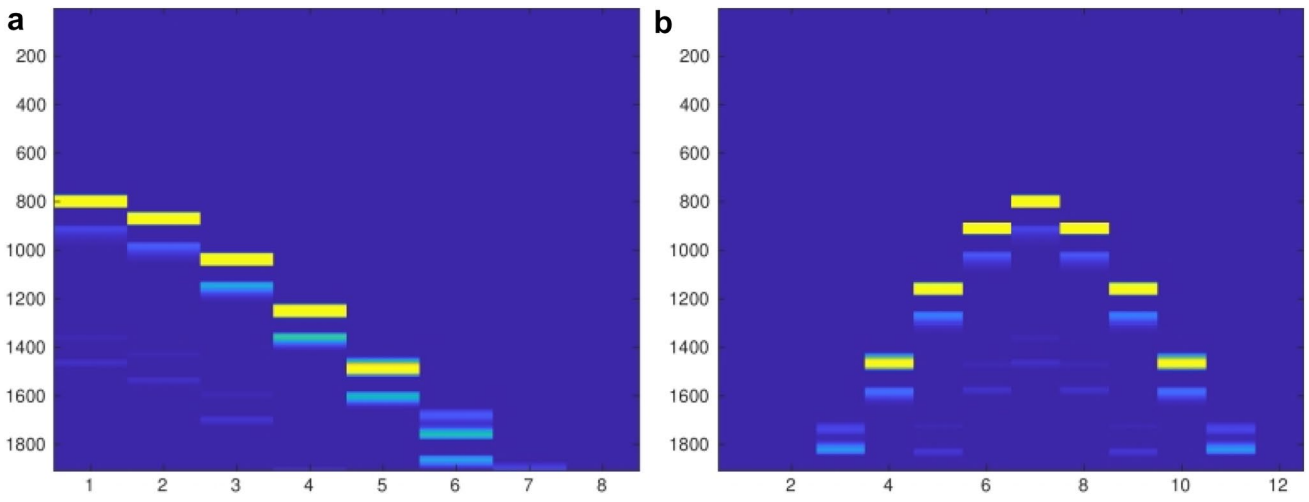

Fig. 7 An example of a radargram (B-scan) from a conventional CMP survey procedure **a** and from a GPRdevice, where transmitter and receiver are unseparable **b**

surface, where the hertzian dipole is moving, is 0.25 m as shown in Fig. 8.

In order to validate the proposed procedure two simulations have been run: once separating transmitter and receiver (CMP) and once simulating a device without any separation between transmitter and receiver. Since the offset between transmitting and receiving antennas in the conventional CMP procedure is not constant, only the incremental step (step size) between the A-scans has been kept constant, in order to compare simulation results with the modified proposed CMP technique. Simulations have been run changing the step size from 0.10 to 0.16m and changing the offset between the transmitting and the receiving antenna. In particular, two different offsets have been considered: 0.008 and 0.02 m. The choice of those values has been dictated by the spatial resolution of the simulation environment in *gprMax*. The step size must be a multiple integer of the spatial resolution of the model (resolution along the x, y and z axis is: 0.002 m) otherwise problems with the simulation results will occur *gprMax*. The choice of a spatial resolution of 0.001 m along all three axes could fix the problem at first (since every positive step size can be a multiple integer of 0.001 m), but the simulation time would increase enormously and the same simulation would take almost one day to finish. For this reason, a resolution of 0.002 m have been used and the step sizes of 0.10, 0.12, 0.14, 0.16 m have been considered.

Once a step size has been defined, all simulations run under the same starting condition: the conventional CMP procedure and the proposed one run with the same step size (e.g., 0.1 m). Then an offset need to be choose, for instance 0.008 m. This offset is the starting offset between transmitter and receiver in the conventional CMP procedure at the position x_0. For the proposed CMP procedure, the offset between both antennas is kept constant, as shown in Fig. 9. With the same simulation setup more simulations were carried out, every time changing the relative permittivity from 3 to 6.

Another consideration should be done regarding the calculation procedure discussed in this paper: in relation to

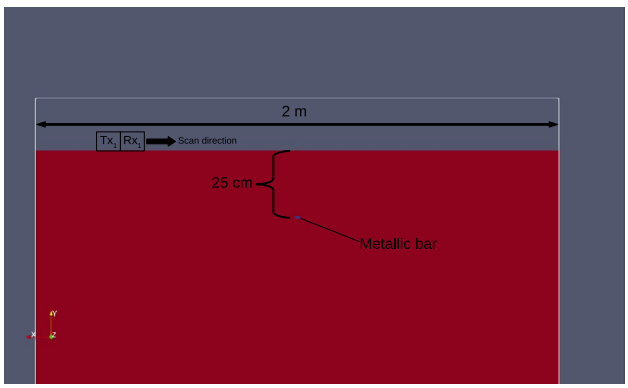

Fig. 8 Simulation environment

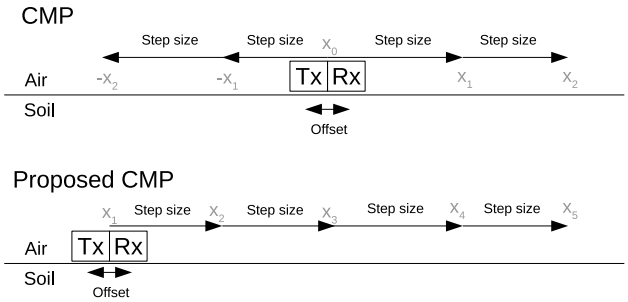

Fig. 9 Conventional and proposed CMP with same step size and, in case of conventional CMP, same start offset between antennas

Figs. 4, 5 is it clear, that the time of flight of a signal is not perfectly symmetrical to the vertical axis. The emitted signal cannot exactly overlap with the reflected signal, if an offset between the antennas is considered. Thus, in reference to Fig. 6, where an ideal model is depicted, the time of flight of the signal t_2 at the position x_2 is slightly different then the time of flight of the signal t_4 at the position x_4. This leads to the problem that reordering the vector t_2 or t_4 must be used (the same is true for the travel paths t_1 and t_5). Thus, an approximation should be taken into account. The method which has been implemented in this research, is simply to mean the values:

$$t_2' = t_4' = \frac{t_2 + t_4}{2} \tag{15}$$

Then the resulting vector will be:

$$\mathbf{CMP_{mod}} = [t_0, t_1', t_2'] = \mathbf{CMP} \tag{16}$$

At this point the electromagnetic properties of the host medium are estimated by the same calculation for conventional CMP procedures. Table 2 shows the electromagnetic parameters of the host medium, which have been implemented in the simulation environment. Only the relative permittivity ε_r is increased by one at every simulation run. All other parameters remain constant.

As already stated above, it is possible to automate part of the simulation process, since the input file for *gprMax* accept some *Python* commands. The simulation outputs the results of the simulated survey in a HDF5 file. The file is then read by a *Matlab*© script, where the ε_r of different host

Table 2 Electromagnetic properties of the host medium

Conductivity (σ)	0
Relative permittivity (ε_r)	$3 \div 6$
Relative permeability (μ_r)	0
Magnetic loss (σ_*)	1

mediums is estimated. Depending on which type of survey has been simulated, the script applies the calculation for the conventional CMP procedure or resorts the vector and then the proposed CMP calculation is applied. The results are reported in Table 3.

The results from Table 3 are plotted in Fig. 10, where a comparison between the conventional CMP and the new sorted vector simulating a GPRdevice is shown.

The same simulation scenery is then repeated after changing the offset value from 0.008 to 0.02 m and the results are reported in the following Table 4.

The results from Table 4 are plotted in Fig. 11, where a comparison between the conventional CMP and the new sorted vector simulating a GPRdevice is shown.

In the tables above (Tables 3, 4) the conventional and the proposed CMP differs from the ideal ε_r in some points more than 10%. Such error in the estimation of ε_r are not unsual (Harry 2009). It is interesting to note, that *both* procedures diverges about almost the same amount at same point from the ideal ε_r, even if they sometime diverges in opposite directions. As stated in Warren et al. (2016), by using a bowtie antenna in simulations would allow to get better and more accurate results. For this reason, the simulated hertzian dipole antenna used in this simulations, need to be replaced in the future by a more accurate antenna model. However, the topic in this paper focused on the comparison of a conventional CMP procedure against the resorted vector collected by a GPRdevice, where transmitter and receiver are unseparable. The comparison shows, that swapping the columns of the vector, as explained above, very similar estimations of the ε_r of the host medium can be achieved.

Table 3 Offset between antennas 0.008 m

Ideal ε_r	Conv. CMP	Modified CMP	Rel. error conv. CMP (%)	Rel. error proposed CMP (%)
3	3.18	3.13	6.00	4.33
4	3.94	3.91	– 1.50	– 2.25
5	4.95	4.84	– 1.00	– 3.20
6	6.40	6.18	6.67	3.00
Step size: 0.12 m				
3	3.09	3.01	3.00	0.33
4	3.80	3.72	– 5.00	– 7.00
5	4.86	4.77	– 2.80	– 4.60
6	5.95	5.56	– 0.83	– 7.33
Step size: 0.14 m				
3	3.02	2.94	0.67	– 2.00
4	3.82	3.87	– 4.50	– 3.25
5	4.32	5.15	– 13.60	3.00
6	5.32	5.28	– 11.33	– 12.00
Step size: 0.16 m				
3	3.09	3.05	3.00	1.67
4	4.30	4.19	7.50	4.75
5	4.40	5.59	– 12.00	11.80
6	6.12	5.93	2.00	– 1.17

Table 4 Offset between antennas 0.02 m

Ideal ε_r	Conv. CMP	Modified CMP	Rel. error conv. CMP (%)	Rel. error proposed CMP (%)
3	3.16	3.11	5.33	3.67
4	3.93	3.91	– 1.75	– 2.25
5	4.85	4.85	– 3.00	– 3.00
6	6.35	6.20	5.83	3.33
Step size: 0.12 m				
3	3.08	3.02	2.67	0.67
4	3.81	3.72	– 4.75	– 7.00
5	4.75	5.28	– 5.00	5.60
6	6.28	6.11	4.67	1.83
Step size: 0.14 m				
3	3.01	3.32	0.33	10.67
4	3.82	3.88	– 4.50	– 3.00
5	5.26	5.15	5.20	3.00
6	5.94	6.29	– 1.00	4.83
Step size: 0.16 m				
3	3.07	3.04	2.33	1.33
4	3.93	3.92	– 1.75	– 2.00
5	5.61	5.59	12.20	11.80
6	6.10	5.93	1.67	– 1.17

5 Results

As shown in Sect. 4 a conventional CMP calculation algorithm can be rearranged and used even if the GPRsystem does not allow for the separation between transmitter and receiver. The difference to a conventional CMP method is that at least one post-processing step should be added. This step consists of reordering the output matrix, in such a way, that symmetrical scans (same distance from a minimum vertical distance to the buried object) are identified and sorted in a vector, as they were taken by a separated transmitter and receiver unit. In this way the assumption of a symmetrical travel path of the radar signal in the host medium can be made and the estimation of the lightspeed in the medium can be calculated with the same algorithms used for the conventional CMP method.

6 Outlook

The scope of this paper is limited to the development and implementation of a working principle of this method. For further validation this process, future research will

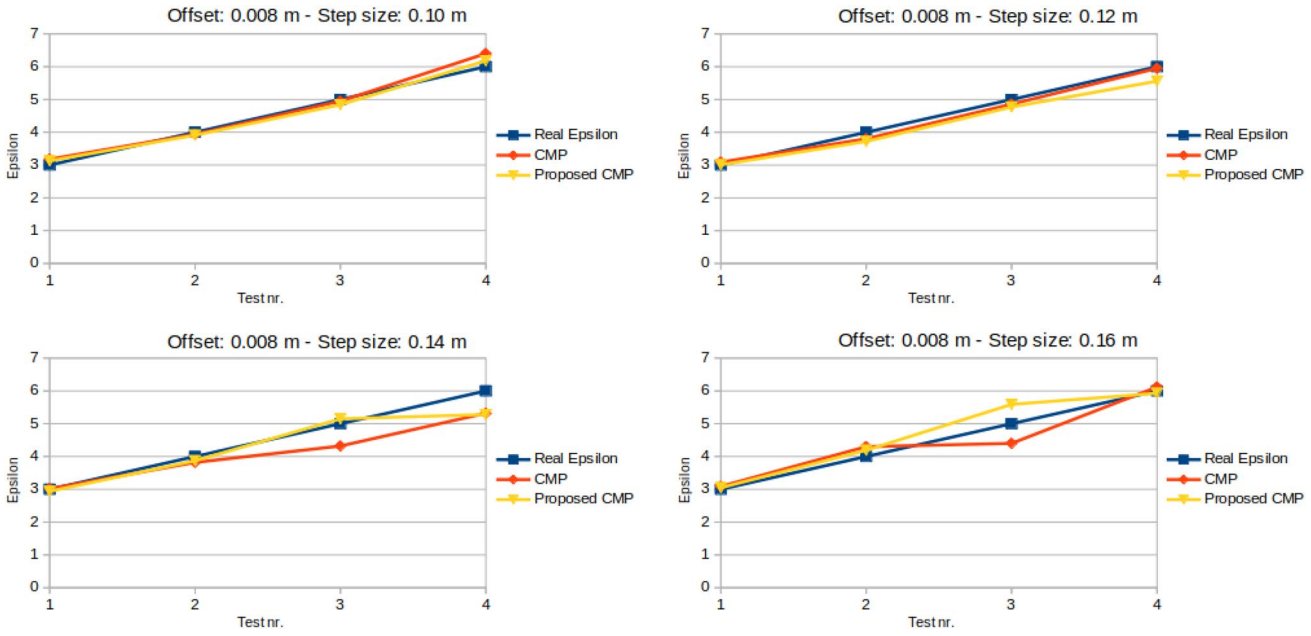

Fig. 10 Comparison of the modified CMP method against the conventional CMP. Offset: 0.008 m

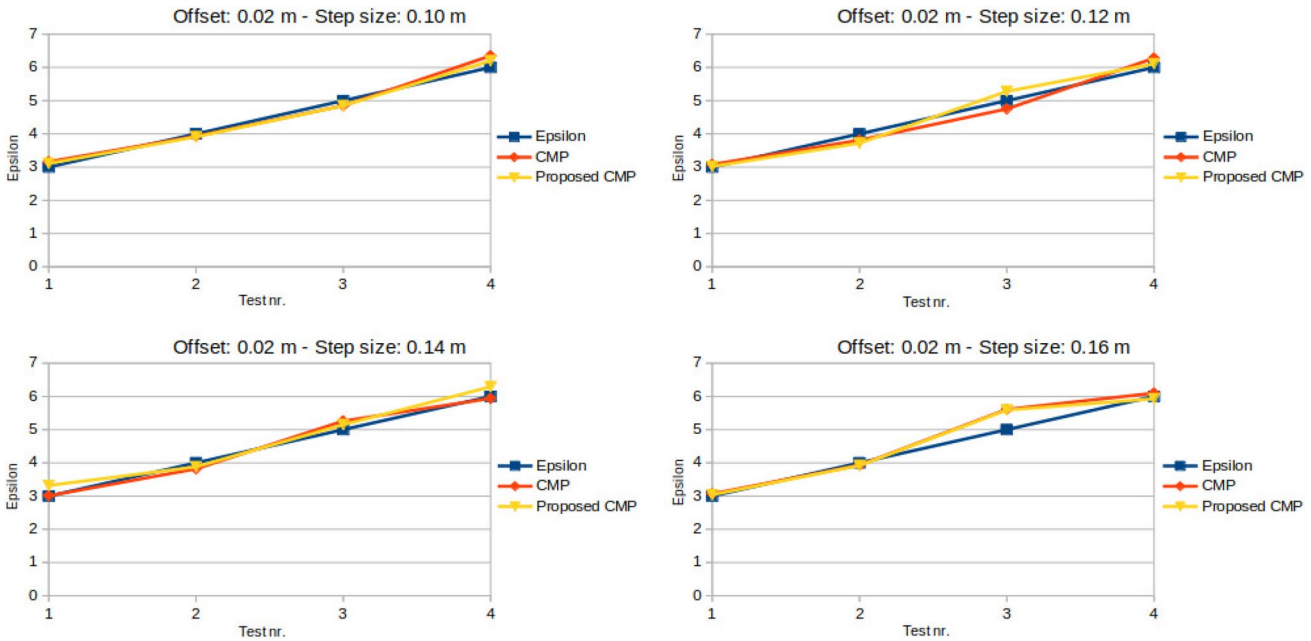

Fig. 11 Comparison of the modified CMP method against the conventional CMP. Offset: 0.02 m

expand upon these developments. For a better evaluation of this procedure more tests and simulations are going to be carried out (for instance, replacing the dipole antenna by a bowtie antenna and implementing different wavelets of the exciting signal). For this purpose, the acquisition of much more powerful hardware and a very good GPU is mandatory. A simple setup like the B-scan example on the website *www.gprmax.com* (*"B-scan with a bowtie antenna model"*) requires almost more than 14 hours using a the actual hardware setup, composed on an AMD Ryzen 7 2700 Eight-Core as a Processor and a GeForce GT 1030 as a graphic card. The present research leads to the possibility of applying the calculations developed for CMP

Fig. 12 Real experiments using a Kuka KMR iiwa mobile platform

Fig. 13 An overview of the Kuka MKR iiwa mobile platform during a scan execution

techniques, to a GPRdevice, in which transmitter and receiver cannot be physically separated.

Furthermore, in the next development step, a real situation is going to be replicated (Fig. 12). The radar scanner is fixed at the robot arm of a mobile platform. The translational movement along the wall of the mobile platform offers the benefit of determining the position of the radar device *at any point x*, since the robot retrieves its position from a starting point using digital encoders. This creates an easy positioning of the radar scanner from a known location.

The x radar position can be retrieved over the existing robot/machine interface and collected for post-processing. Figure 13 shows the process of getting data from wall using the radar scanner and the position of the robot using the mobile platform. The robot uses its force torque sensor to adapt to the uneven surface of the wall while maintaining pressure of sensor against the surface. The safety features of the collaborative robot enables mobile platforms to be used nearby human operators. Further research will investigate the integration of CMP and robotics in real world conditions. The integration of CMP and robotics aims to enable a greater capacity for automated inspection on construction sites.

Acknowledgements This research received funding from Aachener Grundvermögen Kapitalverwaltungsgesellschaft mbH (Köln, Germany) and is filed in the European patent application: PCT/EP2020/068119. All authors have read and agreed to the published version of the manuscript.

Funding Open Access funding enabled and organized by Projekt DEAL.

Declarations

Conflicts of interest The authors declare no conflict of interest.

References

Daniels D J (2005) Ground penetrating radar, John Wiley & Sons Ltd,

Greaves R (2009) Velocity variations and water content estimated from multi-offset, ground-penetrating radar. Geophysics 61(3):683–695. https://doi.org/10.1190/1.1443996

Harry M (2009) Jol. Elsevier Science, Ground Penetrating Radar Theory and Applications

Liang H, Xing L, Lin J (2020) Application and algorithm of ground-penetrating radar for plant root detection: a review. Sensors. https://doi.org/10.3390/s20102836

Persico M (2014) Introduction to ground penetrating radar: inverse scattering and data processing, John Wiley & Sons Ltd

Shan Z, Imad LA (2016) Development of an analytic approach utilizing the extended common midpoint method to estimate asphalt pavement thickness with 3-D ground-penetrating radar. NDT & Int 29–36

Takahashi K (2012) Basics and application of ground-penetrating radar as a tool for monitoring irrigation process, https://www.researchgate.net/publication/221927920https://doi.org/10.5772/29324

Warren C, Giannopoulus A, Giannakis I, gprMax (2016) Open Source software to simulate electromagnetic wave propagation for ground penetrating radar. Comput Phys Commun, https://doi.org/10.1016/j.cpc.2016.08

White R (2020) Regional geology and tectonics volume 1: principles of geologic analysis, Elsevier, Chapter 21"Wide-angle refraction and reflection", https://doi.org/10.1016/C2017-0-00442-1J